The Canadian Mineralogist
Vol. 31, pp. 649-663 (1993)

INTRA- AND INTERCRYSTALLINE CATION-EXCHANGE REACTIONS IN ZONED CALCIC AMPHIBOLE FROM THE BUSHVELD COMPLEX

ANDREW J. ZINGG*

Department of Geology, Rand Afrikaans University, P.O. Box 524, Johannesburg 2000, South Africa, and Department of Geosciences, Mining University, 8700 Leoben, Austria

ABSTRACT

A total of four bulk exchange-vectors are required to describe the compositional range of zoned crystals of calcic amphibole from a mafic pegmatite of replacement origin from the Bushveld Complex, South Africa. Disregarding minor elements, two gross patterns of cation-exchange are distinguished: 1) tremolite exchange: $Ca_2Mg_5Si_8O_{22}(OH)_2 \rightarrow Ca_2Mg_4FeSi_8O_{22}(OH)_2$, and 2) pargasite exchange: $Ca_2Mg_4FeSi_8O_{22}(OH)_2 \rightarrow NaCa_2Mg_2Fe_2AlAl_2Si_6O_{22}(OH)_2$. In the tremolite exchange, the main vector is $FeMg_{-1}$. A small excess of Fe^{2+} is assigned to the $M(4)$ site. Only where Mg/(Mg+Fe) is less than 0.8 is the pargasite component incorporated into the structure along with further replacement of Mg by Fe. Titanium is part of two different elementary vectors, first in $^{VI}\Diamond_{1.67}TiFe^{3+}_{1.33}Mg_{-4}$ until Ti reaches a level of 0.05 apfu, and then in either $TiSi_{-1}$ or $TiAl_2Mg_{-1}Si_{-2}$, depending on whether tetrahedral or octahedral sites are occupied. The reaction responsible for the formation of tremolite-rich amphibole is 2 $Cpx_{0.7}$ + 2 7/8 $Opx_{0.6}$ + 1 1/8 $Ol_{0.5}$ + H_2O + 0.36 $O_2 \rightarrow 1Tr_{0.85}$ + 0.71 Mag. The actual zoning in the amphibole is due to the presence of pargasite and can be expressed by: $Amp_x + b\ Cpx_{0.7} + c\ Opx_{0.6} + d\ Ol_{0.5} + (a-1)\ H_2O + e/2\ O_2 \rightarrow a\ Amp_y + e$ Mag.

Keywords: amphibole, cation mixing, exchange-vector, vacancies, tremolite, edenite, tschermakite, pargasite, mafic pegmatite, Bushveld Complex, South Africa.

SOMMAIRE

Quatre vecteurs d'échange s'avèrent nécessaires pour décrire les variations en composition de cristaux d'amphibole calcique dans une pegmatite mafique produite par remplacement dans le complexe de Bushveld, en Afrique du Sud. Sans considérer les éléments mineurs, deux schémas globaux d'échange cationique semblent importants: 1) échange trémolitique: $Ca_2Mg_5Si_8O_{22}(OH)_2 \rightarrow Ca_2Mg_4FeSi_8O_{22}(OH)_2$, et 2) échange pargasitique: $Ca_2Mg_4FeSi_8O_{22}(OH)_2 \rightarrow NaCa_2Mg_2Fe_2AlAl_2Si_6O_{22}(OH)_2$. Dans l'échange trémolitique, le vecteur d'échange important est $FeMg_{-1}$. Un léger excès de Fe^{2+} est placé sur le site $M(4)$. Dans les cas où le rapport Mg/(Mg+Fe) est inférieur à 0.8, le pôle pargasitique devient important, avec remplacement plus poussé du Mg par le Fe. Le Ti peut faire partie de deux vecteurs élémentaires importants, d'abord $^{VI}\Diamond_{1.67}TiFe^{3+}_{1.33}Mg_{-4}$ jusqu'au point où le Ti atteint un niveau de 0.05 atomes par unité formulaire, et ensuite soit $TiSi_{-1}$ ou $TiAl_2Mg_{-1}Si_{-2}$, selon la coordinence du Ti, tétraédrique ou octaédrique. La réaction responsable de la formation de l'amphibole riche en trémolite serait 2 $Cpx_{0.7}$ + 2 7/8 $Opx_{0.6}$ + 1 1/8 $Ol_{0.5}$ + H_2O + 0.36 $O_2 \rightarrow 1\ Tr_{0.85}$ + 0.71 Mag. La présence de zonation dans l'amphibole est attribuée à la présence du pôle pargasite, et serait exprimée par la réaction $Amp_x + b\ Cpx_{0.7} + c\ Opx_{0.6} + d\ Ol_{0.5} + (a-1)\ H_2O + e/2\ O_2 \rightarrow a\ Amp_y + e$ Mag.

(Traduit par la Rédaction)

Mots-clés: amphibole, mélange de cations, vecteur d'échange, lacunes, trémolite, édenite, tschermakite, pargasite, pegmatite mafique, complexe de Bushveld, Afrique du Sud.

INTRODUCTION

Amphibole-group minerals may host a variety of major (Na, Ca, Mg, Fe^{2+}, Al and Si) and minor elements (K, Fe^{3+}, Ti, Mn, Cr and Li, among others). The elements are distributed according to the following structural formula (Leake 1978, Robinson *et al.* 1982): $A_{0-1}B_2C_5T_8O_{22}W_2$. The A position is usually occupied by Na and K, and may also be partly vacant; the B position [$M(4)$] is occupied by Ca, Na, Li, Fe^{2+}, Mn and Mg, the C position [$M(1,2,3)$], by Mg, Fe^{2+}, Fe^{3+},

**Present address:* Büro für Technische Geologie, 7320 Sargans, Switzerland.

Al, Ti and Li, the *T*[1,2] position, by Si and Al, and the *W* position [O(3)], by O, OH, F and Cl. Whereas individual site-occupancies are generally known from structure refinements (*e.g.*, Colville *et al.* 1966, Papike & Clark 1969, Papike & Ross 1970, Ungaretti *et al.* 1981, Hawthorne 1981, 1983), the coupling of cations during amphibole formation is not well understood. The variation in concentration of cations is subject to constraints of site and charge balance, and is best described in terms of exchange-vectors (Thompson 1981, 1982, Thompson *et al.* 1982, Burt 1988). Results of a single analysis of a mineral provide one point in composition space (Thompson 1982), and a vector to this point can only be established relative to an arbitrarily chosen additive component (*e.g.*, tremolite) as starting composition. The significance of such a vector is questionable. Exchange reactions are dynamic processes, not accessible to direct observation; therefore, true exchange-vectors can only be determined if traces of different stages in the process of formation have been preserved, which is the case for zoned crystals. It is always possible to determine a bulk exchange-vector between two compositionally different points in a zoned crystal. The components *(elementary vectors)* of this bulk vector are not necessarily evident.

The aim of the present study is to determine the type of exchange vectors responsible for the chemical variation of zoned crystals of calcic amphibole from ultramafic rocks of the Bushveld Complex. The study of the Bushveld material shows that from a crystal's core to its rim, only one or two combinations of elementary vectors are realistic. These choices involve common vectors (*e.g.*, the Tschermak substitution or edenite), but may also include unusual ones. The way cations couple is of importance for an understanding of the mixing properties of amphibole solid-solutions. It is proposed that the amphibole crystals studied formed in an equilibrium process. The exchange mechanism will be used to derive continuous reactions among coexisting phases in the Bushveld pegmatite.

Rock Samples and Analytical Techniques

Iron-rich ultramafic (IRUM) pegmatites from the Critical Zone of the Bushveld Complex contain coarse-grained (up to several cm) brown to colorless crystals of amphibole. The pegmatites are considered to be of a replacement origin (*e.g.*, Schiffries 1982, Stumpfl & Rucklidge 1982, Viljoen & Scoon 1985). The main argument for such a hypothesis, among others, is the presence of chromitite seams from the layered sequence that cross-cut transgressive IRUM pegmatites without mechanical disturbance. A detailed investigation was conducted on a pegmatite 50 cm wide from the Brits area (southern Bushveld). The whole-rock composition of the different zones is shown in Table 1, and the mineralogy, in Figure 1a.

TABLE 1. CHEMICAL COMPOSITION OF SAMPLES STUDIED

Sample No.	norite	border zone	center
SiO_2 wt.%	51.90	30.30	42.80
TiO_2	n.d.	3.80	1.48
Al_2O_3	22.85	6.80	2.18
Fe_2O_3	0.29	11.89	5.80
FeO	2.17	30.21	22.99
MnO	n.d.	0.39	0.38
MgO	12.08	13.90	16.20
CaO	10.34	3.36	6.60
Na_2O	2.08	0.28	0.26
K_2O	n.d.	0.10	0.31
H_2O^+	n.d.	0.22	1.21
H_2O^-	n.d.	0.02	0.06
Total	101.71	97.86	100.27
NiO (ppm)	n.d.	159	340
CuO (ppm)	n.d.	25	70

The pegmatite is embedded in a noritic host-rock with about 70% plagioclase and 30% orthopyroxene (opx). In a cross section from border to center of the pegmatite, plagioclase is replaced by ferromagnesian minerals. In the border zone, olivine is the dominant mineral of replacement origin, whereas toward the center it is orthopyroxene (Fig. 1a). Also, in the border zone, whole-rock compositions record a decrease in Na and Al, and an increase in Fe, Mg and Si. Calcium first decreases near the contact, then increases toward the pegmatite's center, where element concentrations reach a constant level. Brown amphibole is stable in the border zone, whereas tremolite is found in the center (Fig. 1a). Zoned amphibole with a dark brown to greenish core and a colorless rim first appears between the border zone and the pegmatite's center, and follows the disappearance of plagioclase from the assemblage (Fig. 1a). Zingg (1991) proposed that the brown amphibole is a product of replacement of feldspar. The disappearance of the feldspar is responsible for the cessation of the formation of brown amphibole and the transformation of brown to colorless amphibole.

Mineral analyses were performed on an ARL SEMQ electron microprobe. The excitation potential was 15 kV, and the specimen current was 20 nA. Intensities of $K\alpha$ X-ray lines were collected over 20 seconds; no volatilization of light elements (*i.e.*, Na) was apparent under these conditions. Natural pyroxenes and amphiboles were used as standards. The precision of the electron microprobe and the variability of the amphibole compositions were estimated by analyzing two immediately adjacent spots within one zone of a crystal. The two compositions were always well within the variability defined by symbol size used to display the results in Figures 2 to 6. The analytical results were converted to mineral formulae

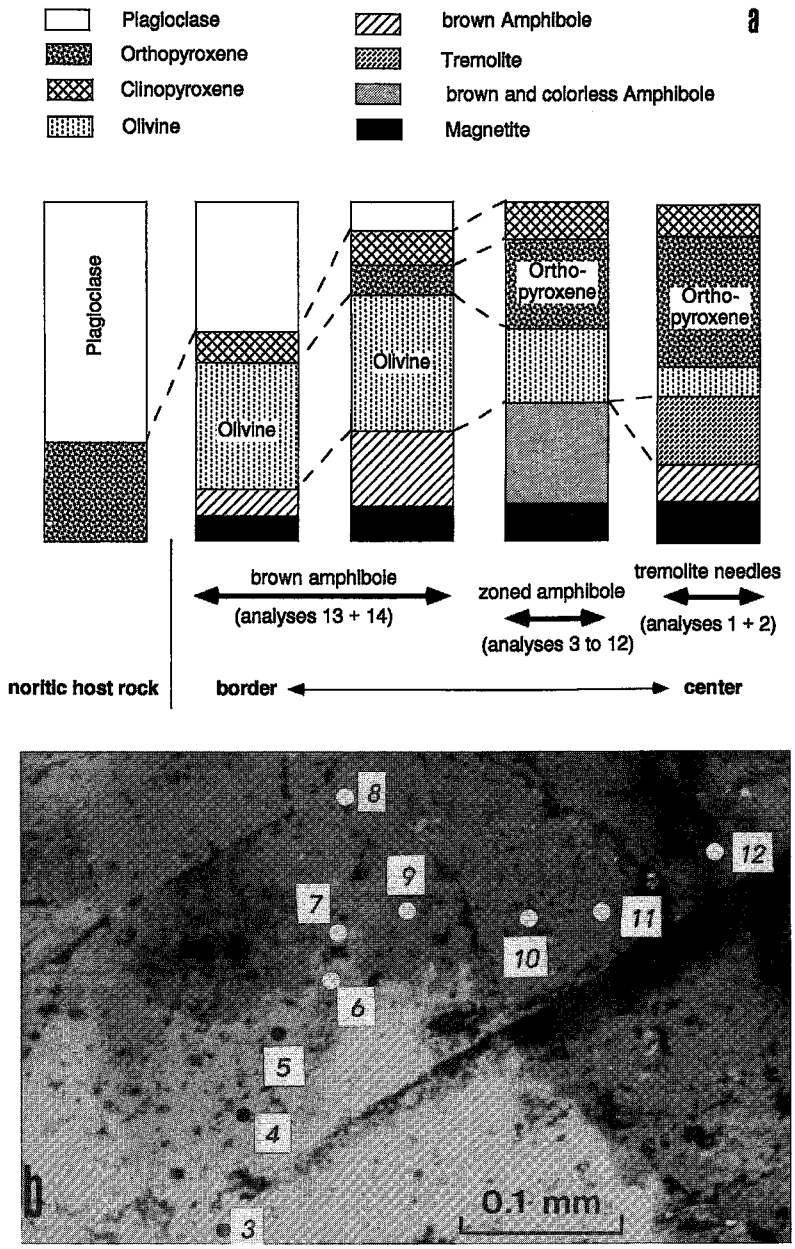

FIG. 1. a. Variation of mineral proportions in a cross section through an iron-rich ultramafic pegmatite in the Bushveld Complex. The disappearance of brown amphibole parallels that of plagioclase and is followed by the appearance of zoned crystals of amphibole. The crystals have a brown core and a colorless rim. The pegmatite center is characterized by tremolite needles. b. Optical micrograph of zoned crystal of amphibole in the pegmatite transition zone showing the spots analyzed (3 to 12).

on the basis of 23 atoms of oxygen per formula unit (pfu). In Table 2, all iron was assumed to be present as FeO, and in Table 3, trivalent iron was estimated assuming a cation sum of 13 excluding Ca, Na and K (Robinson *et al.* 1982). Table 2 shows two compositions (1 and 2) of amphibole from the border zone of the pegmatite (Fig. 1a), ten (3 to 12) from a single zoned grain from the transition zone of the pegmatite (Fig. 1b), and two (13 and 14) of tremolite needles in the center of the pegmatite (Fig. 1a).

TABLE 2. COMPOSITION OF ZONED CRYSTALS OF CALCIC AMPHIBOLE FROM THE BUSHVELD COMPLEX

Sample	1	2	3	4	5	6	7	8	9	10	11	12	13	14
SiO_2	57.36	57.45	54.74	53.11	52.58	51.86	50.93	48.60	47.96	47.55	46.67	44.37	44.55	44.18
TiO_2	0	0	0.08	0.27	0.27	0.40	0.48	0.79	1.30	1.13	1.38	2.18	1.91	2.20
Al_2O_3	0.54	0.67	2.44	4.10	4.75	5.29	6.04	8.58	8.58	9.05	9.72	11.46	11.63	11.88
FeO §	6.01	6.47	9.86	10.54	11.23	11.68	12.06	11.50	12.50	12.57	12.68	13.74	13.88	14.19
MnO	0.13	0.10	0.13	0.14	0.18	0.21	0.19	0.13	0.17	0.17	0.15	0.18	0.16	0.20
MgO	20.69	20.51	17.79	16.58	15.81	15.24	14.61	14.45	13.74	13.76	13.42	11.88	11.78	11.27
CaO	12.81	12.44	12.21	12.17	12.10	12.23	12.17	12.25	12.16	12.02	11.97	11.84	11.80	11.76
Na_2O	0.12	0.11	0.47	0.78	0.92	1.04	1.14	1.57	1.74	1.78	1.89	2.26	2.29	2.42
Total	97.66	97.75	97.72	97.69	97.84	97.95	97.62	97.87	98.15	98.03	97.88	97.91	98.00	98.10
Si	7.972	7.980	7.756	7.572	7.514	7.434	7.347	7.009	6.944	6.896	6.794	6.520	6.539	6.494
[4]Al	0.028	0.020	0.244	0.428	0.486	0.566	0.653	0.991	1.056	1.104	1.206	1.480	1.461	1.506
T-sites	8.000	8.000	8.000	8.000	8.000	8.000	8.000	8.000	8.000	8.000	8.000	8.000	8.000	8.000
[6]Al	0.060	0.089	0.163	0.261	0.314	0.327	0.374	0.467	0.408	0.433	0.462	0.505	0.551	0.552
Ti	0.000	0.000	0.008	0.028	0.029	0.043	0.052	0.085	0.141	0.123	0.151	0.240	0.210	0.243
Fe	0.640	0.655	1.058	1.173	1.269	1.350	1.411	1.328	1.467	1.450	1.458	1.632	1.644	1.713
Mn	0.015	0.011	0.015	0.016	0.021	0.025	0.023	0.015	0.020	0.020	0.018	0.022	0.019	0.024
Mg	4.285	4.245	3.756	3.522	3.367	3.255	3.140	3.105	2.964	2.974	2.911	2.601	2.576	2.468
M(1)-M(3)	5.000	5.000	5.000	5.000	5.000	5.000	5.000	5.000	5.000	5.000	5.000	5.000	5.000	5.000
Ca	1.907	1.851	1.853	1.859	1.852	1.878	1.881	1.893	1.886	1.867	1.867	1.864	1.855	1.852
Fe	0.058	0.096	0.110	0.083	0.073	0.050	0.043	0.059	0.046	0.074	0.085	0.056	0.059	0.031
Na	0.032	0.029	0.037	0.058	0.075	0.072	0.076	0.048	0.068	0.059	0.048	0.080	0.086	0.117
M(4)	1.997	1.976	2.000	2.000	2.000	2.000	2.000	2.000	2.000	2.000	2.000	2.000	2.000	2.000
Na	0.000	0.000	0.092	0.157	0.179	0.217	0.243	0.391	0.420	0.441	0.485	0.563	0.565	0.572
Mg/(Mg+Fe)	0.86	0.85	0.763	0.737	0.715	0.699	0.683	0.691	0.662	0.661	0.654	0.606	0.651	0.689

§ All iron is expressed as FeO. Analyses 1,2: tremolite needles in pegmatite core; 3-12: zoned amphibole in the pegmatite transition zone (Fig. 1); 13,14: brown amphibole coexisting in pegmatite border zone.

TABLE 3. COMPOSITION OF ZONED CRYSTALS OF CALCIC AMPHIBOLE FROM THE BUSHVELD COMPLEX

Sample	1	2	3	4	5	6	7	8	9	10	11	12	13	14
SiO_2	57.36	57.45	54.74	53.11	52.58	51.86	50.93	48.60	47.96	47.55	46.67	44.37	44.55	44.18
TiO_2	0	0	0.08	0.27	0.27	0.40	0.48	0.79	1.30	1.13	1.38	2.18	1.91	2.20
Al_2O_3	0.54	0.67	2.44	4.10	4.75	5.29	6.04	8.58	8.58	9.05	9.72	11.46	11.63	11.88
FeO §	6.01	6.47	9.86	10.54	11.23	11.68	12.06	11.50	12.50	12.57	12.68	13.74	13.88	14.19
MnO	0.13	0.10	0.13	0.14	0.18	0.21	0.19	0.13	0.17	0.17	0.15	0.18	0.16	0.20
MgO	20.69	20.51	17.79	16.58	15.81	15.24	14.61	14.45	13.74	13.76	13.42	11.88	11.78	11.27
CaO	12.81	12.44	12.21	12.17	12.10	12.23	12.17	12.25	12.16	12.02	11.97	11.84	11.80	11.76
Na_2O	0.12	0.11	0.47	0.78	0.92	1.04	1.14	1.57	1.74	1.78	1.89	2.26	2.29	2.42
Total	97.66	97.75	97.72	97.69	97.84	97.95	97.62	97.87	98.15	98.03	97.88	97.91	98.00	98.10
Si	7.935	7.919	7.689	7.521	7.471	7.404	7.321	6.975	6.918	6.850	6.749	6.491	6.507	6.477
[4]Al	0.065	0.081	0.311	0.479	0.529	0.596	0.679	1.025	1.082	1.150	1.251	1.509	1.493	1.523
T-sites	8.000	8.000	8.000	8.000	8.000	8.000	8.000	8.000	8.000	8.000	8.000	8.000	8.000	8.000
[6]Al	0.023	0.028	0.093	0.206	0.266	0.294	0.344	0.427	0.376	0.387	0.405	0.466	0.510	0.530
Ti	0.000	0.000	0.008	0.029	0.029	0.043	0.052	0.085	0.141	0.122	0.150	0.240	0.210	0.243
Fe^{3+}	0.213	0.349	0.399	0.308	0.268	0.188	0.164	0.223	0.179	0.310	0.307	0.211	0.221	0.126
Mg	4.267	4.215	3.725	3.500	3.349	3.243	3.131	3.092	2.954	2.955	2.893	2.591	2.565	2.463
Fe^{2+}	0.482	0.397	0.760	0.940	1.067	1.207	1.285	1.158	1.328	1.205	1.226	1.470	1.474	1.614
Mn	0.015	0.012	0.015	0.017	0.022	0.025	0.023	0.016	0.021	0.021	0.018	0.022	0.020	0.025
M(1)-M(3)	5.000	5.000	5.000	5.000	5.000	5.000	5.000	5.000	5.000	5.000	5.000	5.000	5.000	5.000
Ca	1.899	1.837	1.838	1.847	1.842	1.871	1.874	1.884	1.879	1.855	1.855	1.856	1.847	1.847
Na	0.032	0.029	0.128	0.153	0.158	0.129	0.126	0.116	0.121	0.145	0.145	0.144	0.153	0.153
M(4)	1.931	1.867	1.966	2.000	2.000	2.000	2.000	2.000	2.000	2.000	2.000	2.000	2.000	2.000
Na	0.000	0.000	0.000	0.061	0.095	0.159	0.192	0.321	0.366	0.353	0.384	0.497	0.495	0.535
Mg/(Mg+Fe)	0.898	0.914	0.831	0.788	0.758	0.729	0.709	0.728	0.790	0.710	0.702	0.638	0635	0.604

§ Proportion of trivalent iron estimated on the basis of a cation sum of 13 excluding Ca, Na and K. Analyses 1,2: tremolite needles in pegmatite core; 3-12: zoned amphibole in the pegmatite transition zone (Fig. 1); 13,14: brown amphibole coexisting in pegmatite border zone.

Derivation of Exchange-Vectors

Figures 2 through 6 display correlations between the important cations. A correlation may be either positive, if two cations are incorporated in parallel, or negative, if one cation replaces another. Examples of negative slopes and the replacement of cations are observed for Si *versus* Al^{tot} (Fig. 2), Fe^{tot} *versus* Mg (Fig. 4), and Mg *versus* Ti (Fig. 6). Positive slopes and simultaneous incorporation are observed for $^{[6]}Al$ *versus* $^{[4]}Al$ (Fig. 3), and Na *versus* Al^{tot} (Fig. 5). A linear correlation is suggested by the site-balance criteria; the sum of cations *A* and *B* has to be replaced by an *equal* number of cations *C* and *D*. Linear trends may be interrupted, and slopes may change. Such discontinuities are shown in Figure 4 at Mg = 3.9 atoms pfu (apfu), Fe = 1.1 or in Figure 6 at Mg = 3.2, Ti = 0.05. On either side of the discontinuity, the slopes, and therefore the ratios between different cations, are constant. Between two adjacent discontinuities, it is possible to determine a bulk vector by subtracting the cation concentrations (apfu) at one discontinuity from the cation concentrations (apfu) at the other. Discontinuities occur where the ratio between cations changes owing to the appearance or disappearance of elementary vectors. A comparison of different bulk-vectors between adjacent discontinuities may reveal elementary vectors. Such discontinuities, or intersections of two trends, are important, and key compositions are assigned to them. In general, key compositions do not necessarily coincide with results of an electron-microprobe analysis. If the crystal were continuously zoned, however, then the key compositions should occur.

Another important feature in the cation plots are intercepts. Examples are shown in Figure 3, where $^{[6]}Al$ equals 0.06 at $^{[4]}Al = 0$, or in Figure 6, where Mg = 3.9 at Ti = 0. Intercept values provide information on the point at which a cation starts to be incorporated in terms of another component. A discontinuity in one diagram may coincide with an intercept in another. Both witness the appearance of a new elementary vector.

The position of a key composition is subject to uncertainty. It may be shifted within the uncertainty range of the linear trends on either side of the discontinuity to match the constraints imposed by the vectors. This has no effect on the type of exchange-vectors. However, the shift augments the size of the elementary vector on one side of the discontinuity and diminishes it on the other. Problems in deriving elementary vectors exist if cation contents (*e.g.*, Fe^{3+}) or vacancies

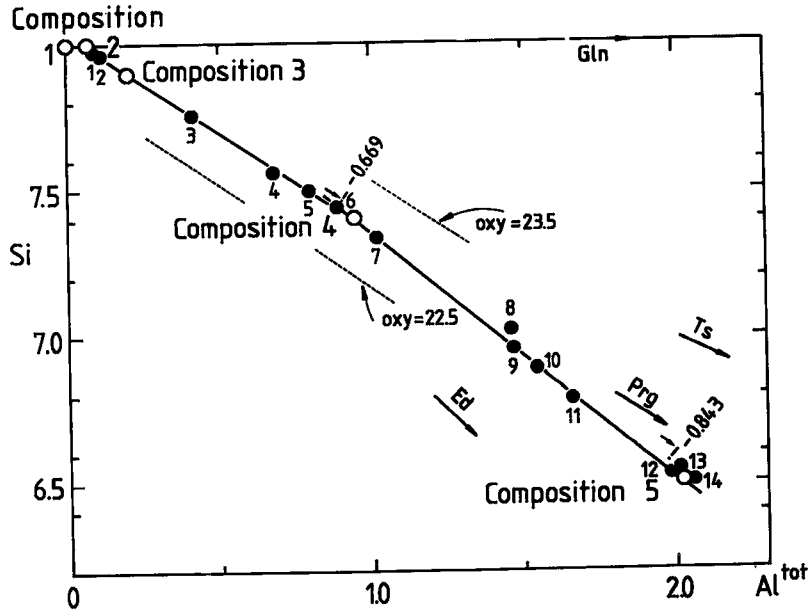

FIG. 2. Si *versus* Al in Bushveld suite of amphibole compositions. Key compositions are shown by open symbols. Two trends are distinguished; one for compositions 1 to 6, the other for compositions 7 to 14. The dashed lines labeled oxy = 22.5 and oxy = 23.5 show the least-square-fitted lines to the data points obtained on the basis of 22.5 and 23.5 oxygen units, respectively. Also shown are the glaucophane (**Gln**), Tschermak (**Ts**), pargasite (**Prg**) and edenite (**Ed**) vectors. The 3-digit numbers at samples 6 and 12 give the slopes obtained by least-squares regression. The correlation coefficient for samples 1–6 is 0.998, and for 7–14, it is 0.995.

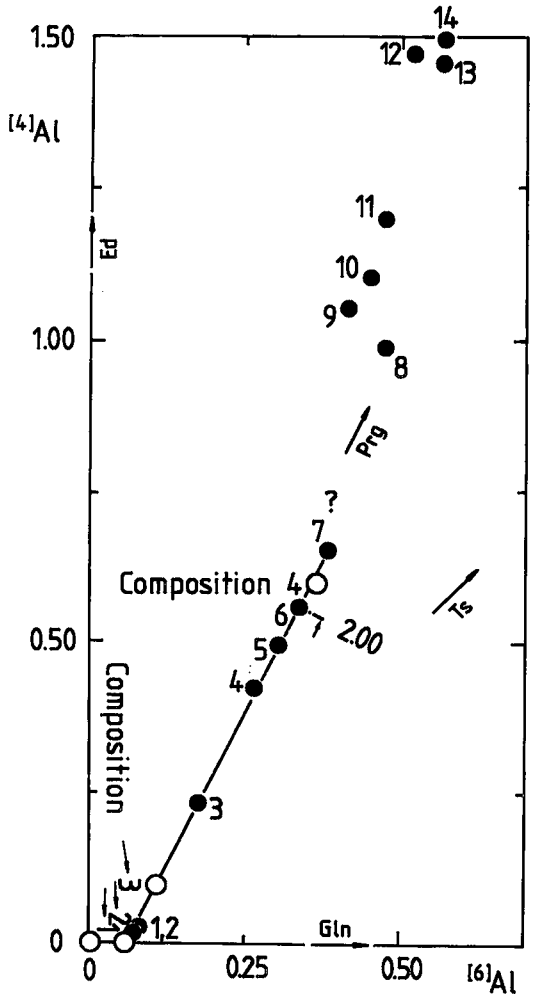

FIG. 3. Proportion of $^{[4]}Al$ *versus* that of $^{[6]}Al$ in Bushveld suite of amphibole compositions. A well-defined slope of 2.00 (compositions 1–6), and intercept value of 0.06 apfu are obtained for samples 1 to 6. Samples 7 to 14 show more scatter. Also displayed are the four vectors given in Figure 2. The correlation coefficient for samples 1–6 is 0.982, and for 7–14, it is 0.833.

cannot be determined with the electron microprobe. This problem can be neglected if the starting key composition is simple and well defined. Examples for such starting compositions are pure cummingtonite or tremolite. In favorable cases, the amount of Fe^{3+} or vacancies can be estimated from site and charge-balance criteria. Whereas the determination of bulk vectors between key compositions is straightforward within the uncertainty ranges of key compositions, and in terms of the cations that can be measured with the electron microprobe, the way they are subdivided into elementary vectors may be debated. The choice of elementary vectors is normally limited. A choice other than the simplest in general would complicate the exchange process proposed dramatically. In the present study, different elementary vectors have been explored; only one or two cases were finally found to be acceptable. These are based on the following principles: a) conventional vectors are chosen to coincide with those generally accepted among investigators of amphibole-group minerals, b) the number of elementary vectors is kept as small as possible, and c) elementary vectors are supposed to show as continuous a pattern as possible from amphibole core to rim.

For the chemical characterization of the zoned crystals of amphibole from the Bushveld complex, five key compositions are required. It will be assumed that trivalent iron is absent in pure tremolite, which will be key composition 1. It is important to note that the following derivation is based on 23 atoms of oxygen. A change in the number of oxygen atoms will alter the intercepts, but not the slopes, as shown for two examples in Figures 2 and 4. A change in the number of oxygen atoms will therefore not affect the type of elementary vectors.

RESULTS FOR THE ZONED AMPHIBOLE CRYSTALS FROM THE BUSHVELD COMPLEX

Cation variation for the zoned amphibole crystals is shown in Figures 2 to 6. Five key compositions allow for four bulk exchange-vectors. In the following sections, each step between adjacent key-compositions will be discussed, and elementary vectors derived. In Figures 2 to 6, slope and intercept values were obtained using least-squares regression analysis. The correlation coefficients are given in the figure captions.

Key composition 1 to 2

The compositions in Table 2 show that the amphibole closest to tremolite (1 and 2) contains Na (0.03 apfu), Mn (0.02) and Al (0.09) in small amounts. Silicon ($\approx$ 7.98) and Ca (1.90) do not attain the theoretical values of 8.0 and 2.0 for pure tremolite. Two key compositions are distinguished: a hypothetical starting composition of pure tremolite, and a second composition obtained from Figures 2 and 3. Both figures show that $^{[4]}Al$ and $^{[6]}Al$ are not coupled until $^{[6]}Al$ reaches 0.06 apfu (intercepts in Figure 2 and 3). Tetrahedrally coordinated aluminum starts to be incorporated only if $^{[6]}Al$ exceeds 0.06. It is important to note that this value is sensitive to changes in the ratio O:OH.

Key composition 2 is defined where $^{[6]}Al = Al^{tot} =$ 0.06 apfu, and silicon is assigned a value of 8.00. The actual value of Si is 7.98; a value of 8.00 is within the

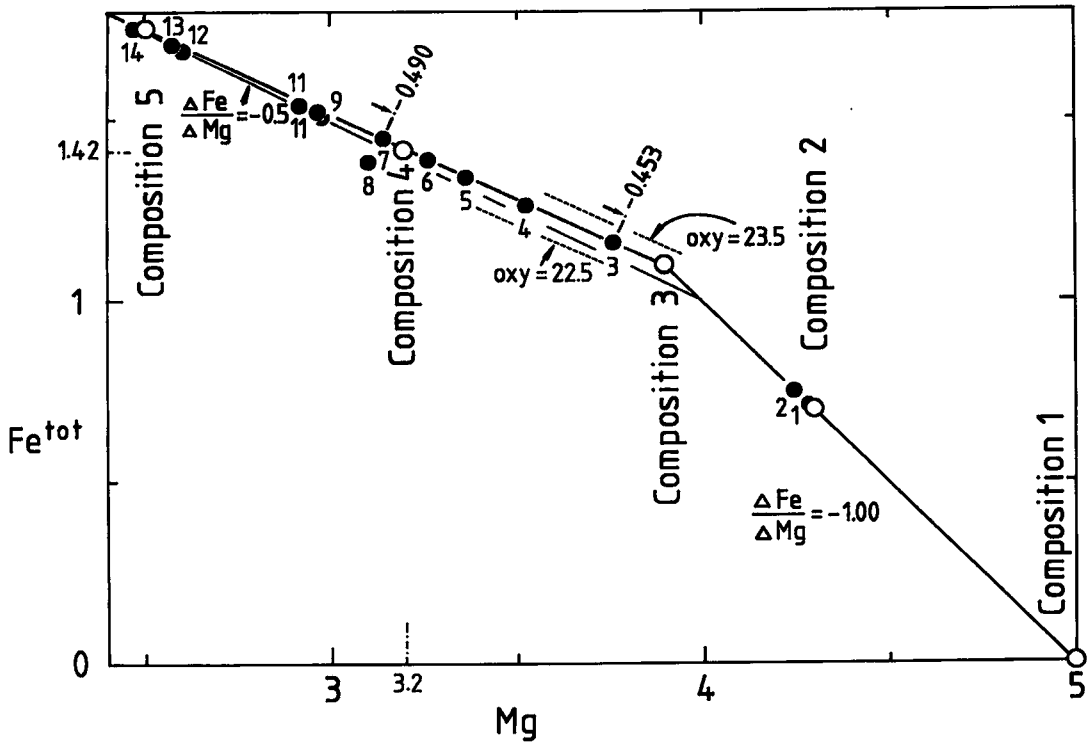

FIG. 4. Proportion of Mg *versus* that of Fe^{tot} in Bushveld suite of amphibole compositions. Two trends are distinguished; one is for compositions 3 to 14, with a slope of roughly –0.5. The second is projected from the origin of vector space (Mg = 5, Fe = 0) through samples 1 and 2, and has a slope of –1.00. Also shown are the least-squares slopes obtained for the oxygen basis of 22.5 and 23.5. Key composition 3 is located at the intersection of these two trends. The correlation coefficient for samples 3–14 is 0.981.

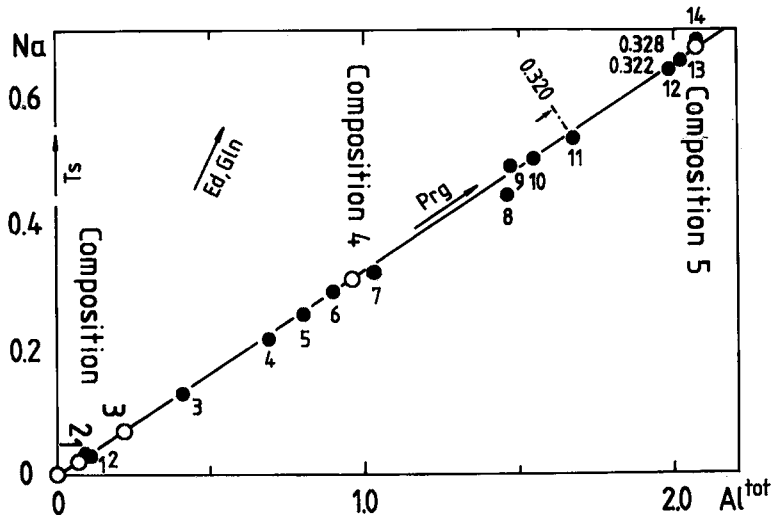

FIG. 5. Na *versus* Al in Bushveld suite of amphibole compositions. All points define a well-defined trend with a slope of about 0.33 and intersecting the origin. The correlation coefficient for samples 1–6 is 0.999, whereas that for all data points is 0.997.

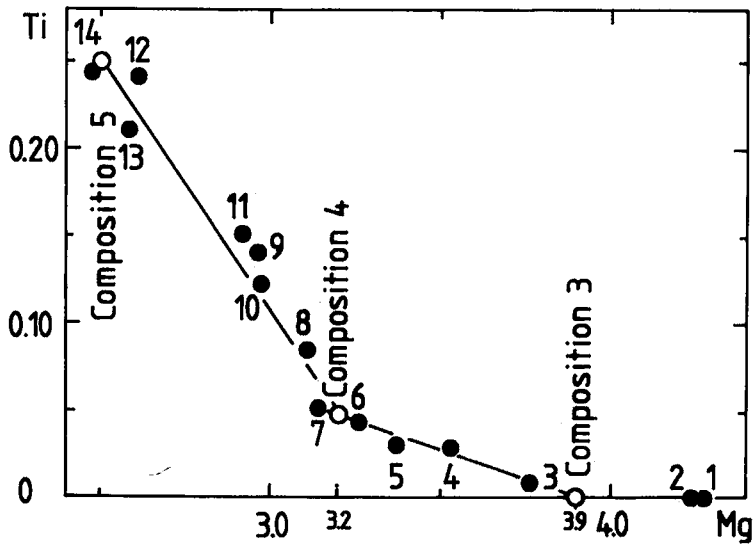

FIG. 6. Ti *versus* Mg in Bushveld suite of amphibole compositions. Two trends are distinguished, a first one for compositions 3 to 6, and a second one, steeper, for compositions 7 to 14. Titanium starts to be incorporated at Mg = 3.9. The correlation coefficient for samples 3–6 is 0.928, whereas that for 7–14 is 0.944.

TABLE 4. KEY COMPOSITIONS AND EXCHANGE VECTORS IN ZONED CRYSTALS OF AMPHIBOLE FROM THE BUSHVELD COMPLEX

Key Composition 1 :	$Ca_2Mg_5Si_8O_{22}(OH)_2$
Exchange Vectors :	0.70 FeMg$_{-1}$ (+ 0.02 Na + 0.02 Mn + 0.06 Al + 0.10 Ca)
Key Composition 2 :	$Na^{M4}_{0.02}Ca_{1.90}Fe^{M4}_{0.08}Mg_{4.30}Fe_{0.62}Mn_{0.02}{}^{[VI]}Al_{0.06}Si_{8.00}O_x(OH)_y$
Exchange Vectors :	0.35 FeMg$_{-1}$, 0.05 FeCa$_{-1}$, 0.05 NaAl□$_{-1}$Si$_{-1}$, 0.05 AlAlMg$_{-1}$Si$_{-1}$
Key Composition 3 :	$Na^{A}_{0.05}Na^{M4}_{0.02}Ca_{1.85}Fe^{M4}_{0.13}Mg_{3.90}Fe_{0.97}Mn_{0.02}{}^{[VI]}Al_{0.11}Si_{7.90}{}^{[IV]}Al_{0.10}O_x(OH)_y$
Exchange Vectors :	0.25 FeMg$_{-1}$, 0.25 NaAl□$_{-1}$Si$_{-1}$, 0.25 AlAlMg$_{-1}$Si$_{-1}$, 0.05 $\Diamond_{1.67}TiFe^{3+}_{1.33}Mg_{-4}$
Key Composition 4 :	$Na^{A}_{0.30}Na^{M4}_{0.02}Ca_{1.85}Fe^{M4}_{0.13}Mg_{3.20}Fe_{1.22}Mn_{0.02}Fe^{3+}_{0.07}{}^{[VI]}Al_{0.36}{}^{[VI]}Ti_{0.05}\Diamond_{0.08}Si_{7.40}{}^{[IV]}Al_{0.60}O_x(OH)_y$
Exchange Vectors :	0.35 FeMg$_{-1}$, 0.35 NaAl□$_{-1}$Si$_{-1}$, 0.35 AlAlMg$_{-1}$Si$_{-1}$, 0.20 TiSi$_{-1}$
Key Composition 5:	$Na^{A}_{0.65}Na^{M4}_{0.02}Ca_{1.85}Fe^{M4}_{0.13}Mg_{2.50}Fe_{1.57}Mn_{0.02}\ Fe^{3+}_{0.07}{}^{[VI]}Al_{0.71}{}^{[VI]}Ti_{0.05}{}^{[IV]}Ti_{0.20}Si_{6.50}{}^{[IV]}Al_{1.30}O_x(OH)_y$
Exchange Vectors :*	0.35 FeMg$_{-1}$, 0.35 NaAl□$_{-1}$Si$_{-1}$, 0.15 AlAlMg$_{-1}$Si$_{-1}$, 0.20 TiAl$_2$Mg$_{-1}$Si$_{-2}$
Key Composition 5 **:	$Na^{A}_{0.65}Na^{M4}_{0.02}Ca_{1.85}Fe^{M4}_{0.13}Mg_{2.50}Fe_{1.57}Mn_{0.02}\ Fe^{3+}_{0.07}{}^{[VI]}Al_{0.51}{}^{[VI]}Ti_{0.25}Si_{6.50}{}^{[IV]}Al_{1.50}O_x(OH)_y$

* Owing to space limitations, vacancies are listed only in the exchange vectors and not in the key compositions. ** Assuming octahedrally coordinated Ti.

range of uncertainty (±0.02). Figure 5 suggests that the ratio between Na and Al is 1:3 over the entire range of compositions; therefore, Na is equal to 0.02 ($Al^{tot}/3$) for key composition 2. The concentration of manganese shows minor fluctuations for all samples and is assigned a value of 0.02. Its constant value suggests that Mn is not involved in the cation-exchange process. The amount of Mg present in key composition 2 is obtained from the intercept in a diagram of Si *versus* Mg. The diagram is not shown owing to some scatter of the data points. Despite the scatter, the diagram allows the determination of the intercept value for Mg, which is 4.30 at Si = 8.00. The amount of divalent iron is provided by Figure 4. According to the figure, pure tremolite and compositions 1 and 2 are connected by a line that has a slope $\Delta Fe/\Delta Mg$ of precisely –1.00. Thus, Mg is replaced by an equal amount of Fe between key compositions 1 and 2, and Fe^{2+} is equal to 0.70 in key composition 2. The postulated straight line between key composition 1 and 2 is not supported by any data points. Deviations from this line, however, would dramatically complicate the postulated exchange-process. There is no evidence for any substantial deviation from the 1:1 slope, as other cations, required for other elementary vectors, are present in trace amounts only. As the $FeMg_{-1}$ exchange is the major one between key composition 1 and 2, even a small deviation would require other cations to participate. The presence of trivalent iron in amphibole 1 and 2 (Table 3) would cause substantial departure from the 1:1 slope and would require a more complex mechanism of exchange. The presence of trivalent iron in these normalized compositions is rejected.

Silicon (8.00 apfu) fills all the tetrahedrally coordinated sites, and Al (0.06 apfu) is entirely confined to the octahedral sites. Magnesium (4.30), Mn (0.02) and Fe (0.62) fill the remaining octahedral sites. Excess Fe (0.08) is placed in the *M*(4) sites (Goldman & Rossman 1977), together with Ca (1.90) and Na (0.02). The cation sum on *M*(4) equals 2.00 apfu. The total positive charge is 46.04, and the ratio O:OH is 22.04:1.96. It seems unreasonable to derive a single exchange-vector between key compositions 1 and 2 on the basis of the minor elements, because such a vector would be highly speculative and uncertain. This is not the case for the major cations Mg^{2+} and Fe^{2+}, where the exchange-vector 0.70 $FeMg_{-1}$ is proposed (Table 4).

Key composition 2 to 3

The one-to-one replacement of Mg by Fe is assumed to continue to key composition 3, which is defined by the intersection of the two linear trends in Figure 4, as well as by the first appearance of Ti (Fig. 6), which starts to be incorporated in key composition 3. Mg equals 3.90 apfu (Figs. 4, 6), yielding Fe = 1.10. Similar to the previous interval (key composition 1 to 2), the 1:1 replacement of Mg by Fe between key composition 2 and 3 is only supported by two data points (1 and 2). A deviation would complicate the exchange process.

Between key compositions 2 and 3, $^{[4]}Al$ and $^{[6]}Al$ are incorporated in the ratio 2:1 (Fig. 3); the ratio Na:Al is 1:3 (Fig. 5). These ratios are consistent with the pargasite (**Prg**) vector, which is the vector sum of equal amounts (= *x*) of edenite (**Ed**) and Tschermakite (**Ts**)

Ed:	*x*	$NaAl\square_{-1}Si_{-1}$
+ Ts:	*x*	$\underline{AlAlMg_{-1}Si_{-1}}$
= Prg:	*x*	$NaAl_3\square_{-1}Mg_{-1}Si_{-2}$

In addition, the $FeMg_{-1}$ exchange-vector is still present as

$$y\ FeMg_{-1}$$

To maintain an overall 1:1 substitution of Mg by Fe (Fig. 4), a fourth exchange-vector is required that provides Fe in the same proportions as the Tschermak exchange removes Mg (= *x*). One vector that can accomplish this is

$$0.05\ FeCa_{-1}$$

which, when applied, causes Ca to drop from 1.9 (key composition 2) to 1.85 (key composition 3). Consistent with these are results of electron-microprobe analyses 2 to 5, which show Ca-values around 1.85. It follows that Mg = 3.9, Fe = 1.1, $^{[6]}Al$ = 0.11 (0.06 + *x*), $^{[4]}Al$ = 0.10 (2**x*), Si = 7.90 (8.00 – 2**x*), Ca = 1.85 (1.90 – *x*), Na = 0.07 (0.02 + *x* or $Al^{tot}/3$), and Mn = 0.02. The value of *y* is 0.35 (Table 4).

Key composition 3 to 4

Key composition 4 is defined by intersections in Figures 2 and 6 and is placed between compositions 6 and 7. A precise position of key composition 4 is not required, as a minor shift will not affect the type of elementary vectors. The bulk vector from key composition 3 to 4 is

$$0.05\ TiNa_5Fe_{6.4}Al_{15}Mg_{-14}Si_{-10}$$

or $\Delta Ti = 0.05$, $\Delta Na = 0.25$, $\Delta Mg = -0.70$, $\Delta Fe = 0.32$, $\Delta Al = 0.75$, and $\Delta Si = -0.50$.

Figures 3 and 5 show a ratio $^{[4]}Al$:$^{[6]}Al$ of 2.00 and Na:Al of 0.32, respectively, consistent with the pargasite vector. Subtracting 0.25 **Prg** (0.25 ΔNa or 0.75 ΔAl^{tot}) from the above bulk vector

$$0.05\ TiNa_5Fe_{6.4}Al_{15}Mg_{-14}Si_{-10}$$
$$-\ 0.25\ NaAl_3Mg_{-1}Si_{-2}$$

leaves the remaining vector

$$0.05\ TiFe_{6.4}Mg_{-9}.$$

Mg is also still replaced by Fe, according to:

$$y\ FeMg_{-1}.$$

The slope $\Delta Fe/\Delta Mg$ in Figure 4 between key compositions 3 and 4 equals –0.453. If the slope were 0.50, y would equal 0.25, and the **Prg** and $FeMg_{-1}$ vectors would be present in equal proportions. The difference (–0.5 *versus* –0.453) in slope may be explained by the presence of Ti, which has not been taken into account so far and which appears for the first time with key composition 3 (Fig. 6). The appearance of Ti is not reflected in Figures 2, 3 (between key compositions 3 and 4) and 5; therefore, Na, $^{[4]}Al$, $^{[6]}Al$ and Si are probably not influenced by and are not part of a vector including Ti. If $y = 0.25$, Mg and Fe would be 3.40 (3.90 – 0.50) and 1.35 (1.10 + 0.25), respectively. According to Figure 4, Fe would be too low by 0.07 apfu (Fe = 1.42 ± 0.01), and Mg, too high by 0.20 apfu (Mg = 3.20 ± 0.01). These values combine with 0.05 apfu of Ti (Fig. 6), suggesting a vector of

$$0.05 \diamond_{3-q} Ti_1 Fe_q Mg_{-4},$$

which is the difference between

$$0.05\ TiFe_{6.4}Mg_{-9}$$

and

$$0.25\ FeMg_{-1}.$$

The symbol ◇ is introduced to indicate a vacancy in the octahedrally coordinated site, in contrast to an

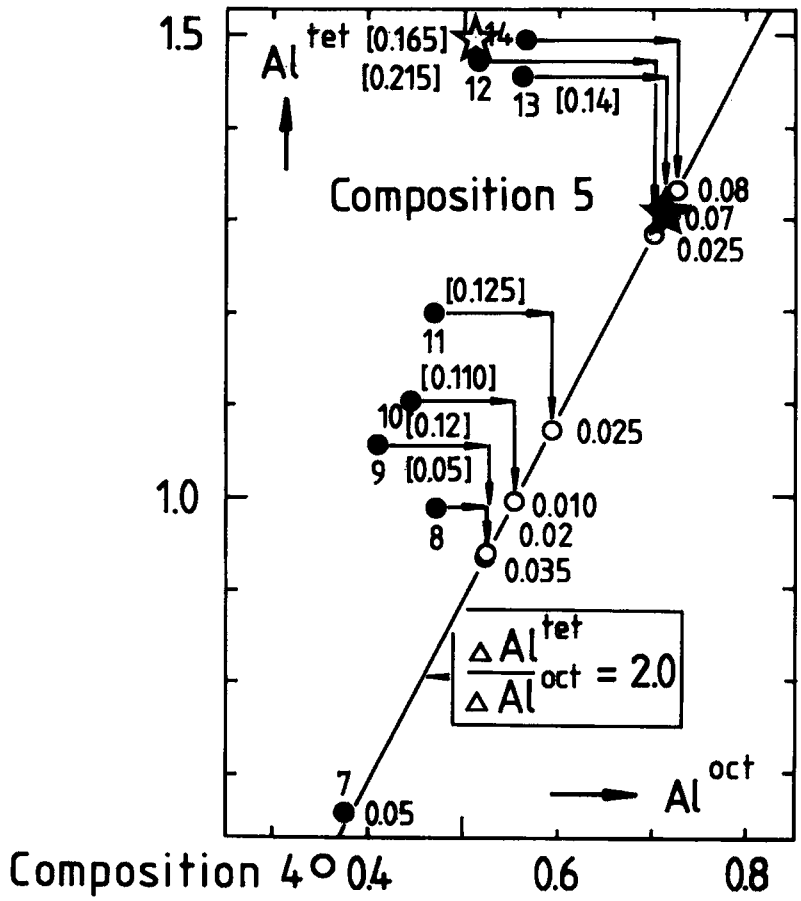

FIG. 7. Shift of data points in Figure 3 if Ti is assigned to tetrahedrally coordinated sites. Numbers in brackets represent reduction of $^{[4]}Al$ and increase of $^{[6]}Al$ if Ti is tetrahedrally coordinated. After this redistribution, the amount of Ti remaining in octahedral sites is given by the numbers accompanying the open circles. The open star symbol shows the position of key composition 5 if Ti is octahedrally coordinated. The filled star symbol records the location of key composition 5 if Ti is tetrahedrally coordinated.

A-site vacancy (□). Such a vacancy is required by the site occupancy. To make up for the difference in Fe of 0.07, q, a parameter not yet defined in the above vector, would have to be 1.4. This latter value has two disadvantages. It requires the introduction of 0.08 octahedral vacancies and a change in the ratio O/OH, as the vector is not charge-balanced. With $q = 2.0$, the vector is charge-balanced; however, a value of 2.0 would lead to $Fe^{2+} = 1.45$. This latter value would disagree considerably with the trend shown in Figure 4. If vacancies are to be avoided, q must have a value of 3.0, resulting in a total iron content of 1.50 (1.35 in key composition 3 + 0.15), which would be too high by 0.08 apfu. If q equals 1.33, which falls within the value of 1.40 ± 0.2 postulated before, and divalent iron is replaced by trivalent iron, the charge is balanced and a change in the O/OH ratio is unnecessary. The proposed vector, therefore, is

$$0.05\ \diamondsuit_{1.67}Ti_1Fe^{3+}_{1.33}Mg_{-4}.$$

The number of octahedral vacancies created is 0.083. A vector combining Ti and octahedral vacancies has been postulated for pyroxene (Gasparik 1985). Ti could also be introduced by the Ti-Tschermak vector:

$$0.05\ TiAl_2Mg_{-1}Si_{-2}.$$

Subtraction of this from the bulk vector between key composition 3 and 4 yields:

$$0.05\ Na_5Fe_{6.4}Al_{13}Mg_{-13}Si_{-8}.$$

This vector cannot be subdivided into conventional elementary vectors without obtaining unrealistic "trash" vectors. The four vectors proposed are the only ones possible without dramatically complicating the exchange process proposed. To summarize, four elementary vectors are required in going from key composition 3 to 4, which are the ones previously proposed:

$$0.25\ \mathbf{Ed} + 0.25\ \mathbf{Ts} + 0.25\ FeMg_{-1}$$

and the new vector:

$$0.05\ \diamondsuit_{1.67}TiFe^{3+}_{1.33}Mg_{-4}.$$

Key composition 4 to 5

Key composition 5 is placed along the line established by analyses 7 to 14. A convenient location is Si = 6.5, $Al^{tot} = 2.0$ (Fig. 2); at $Al^{tot} = 2.0$, Na equals 0.67 (Al/3, Figure 5). According to Figure 4, Mg equals 2.5, and Fe is 1.77. Compared to key composition 4, the changes in the different cations in composition 5 are $\Delta Na = +0.35$, $\Delta Al = +1.05$, $\Delta Si = -0.90$, $\Delta Mg = -0.70$, $\Delta Fe = +0.35$, $\Delta Ti = +0.20$. Two alternative sets of vectors are proposed, with Ti occupying either octahedral or tetrahedral sites.

	tetrahedral Ti	octahedral Ti
Ed	$0.35\ NaAl□_{-1}Si_{-1}$	$0.35\ NaAl□_{-1}Si_{-1}$
Ts	$0.35\ AlAl(MgSi)_{-1}$	$0.15\ AlAl(MgSi)_{-1}$
$FeMg_{-1}$	$0.35\ FeMg_{-1}$	$0.35\ FeMg_{-1}$
Ti-vector	$0.20\ TiSi_{-1}$	$0.20\ TiAlMg_{-1}Si_{-2}$

The exchange-vector $TiSi_{-1}$ was postulated a decade ago by Thompson (1981), and its validity has been debated (Hartman 1969, Ungaretti 1980, Hawthorne 1981, Wagner & Velde 1986, Waychunas 1987, Della Ventura *et al.* 1991). The assignment of Ti to tetrahedral sites would allow the pargasite exchange to continue up to key composition 5. It keeps the number of elementary vectors at a minimum and guarantees the continuation of the exchange pattern observed between key compositions 3 and 4. Figure 3 was constructed with the assumption that Ti is octahedrally coordinated. If Ti is assigned to tetrahedrally instead of octahedrally coordinated sites, the $^{[6]}Al/^{[4]}Al$ ratio will change. The data points of analyses 8 to 14 shift to the **Prg** line, as shown in Figure 7. Residual values of Ti on octahedral sites fluctuate around 0.05, which corresponds to the Ti-concentration of key composition 4. The basic question is, which of the two amphiboles is more stable? Is the influence of Ti large enough to destabilize the pargasite exchange?

Intracrystalline Reactions

The gross exchange of cations in the amphibole crystals from Bushveld follows a simple pattern. In tremolite, with a ratio Mg/(Mg+Fe) between 1.0 to 0.8, Mg is replaced by an equal proportion of Fe. The pattern of 1:1 replacement is not strongly supported by compositional data; however, a different scheme of replacement would dramatically complicate the proposed mechanism of exchange. The overshoot of key composition 3 (Fig. 4) past the point Mg = 4.0 and Fe = 1.0 is worthy of note. A difference of 0.10 in Mg (3.90) and Fe (1.10) allows the presence of 0.05 exchange units of cummingtonite, pargasite and $FeMg_{-1}$. The 0.10 overshoot also allows the presence of octahedrally coordinated Ti and trivalent iron between key compositions 3 and 4. From Table 4, it can be inferred that pargasite and Ti start to be incorporated into the structure once Mg equals 4.0 and Fe equals 1.0. The three vectors **Ed**, **Ts** and $FeMg_{-1}$ are present in equal proportions from the point Mg = 4.0, Fe = 1.0 up to key composition 4 and, depending on whether Ti is assigned to tetrahedral sites or not, possibly also up to key compositions 5. Theoretically, the most Fe-rich amphibole is located at Mg/(Mg+Fe) = 0.5, with an end-member composition $NaCa_2Mg_2Fe_2AlAl_2Si_6O_{22}(OH)_2$, disregarding the presence of minor cations. The simplest process of exchange possible between composition $Ca_2Mg_4FeSi_8O_{22}(OH)_2$ and key composition 5 requires two exchange-vectors only at a time. With Ti

on tetrahedral sites the three elementary vectors

Ed: $NaAl\square_{-1}Si_{-1}$
Ts: $AlAl(MgSi)_{-1}$
and $FeMg_{-1}$

are present in equal proportions over the entire range of composition. The combined vector

$$NaFeAl_3\square_{-1}Mg_{-2}Si_{-2}$$

is coupled with either of the three remaining vectors

$$FeCa_{-1},\ \diamond_{1.67}Fe_{1.33}TiMg_{-4} \text{ and } TiSi_{-1}.$$

If Ti is assigned to octahedrally coordinated sites, the pattern gets more complicated, as the three vectors **Ed**, **Ts** and $FeMg_{-1}$ are no longer present in equal amounts between key compositions 4 and 5.

Whether the postulated mechanism of exchange is general or unique to the Bushveld examples is not known, and might depend on the other minerals present and the conditions of formation. There are no published data available on calcic amphiboles. Stout (1971) suggested that aluminous cummingtonite from Telemark, Norway first obeys a 1:1 replacement of Mg by Fe between $Mg_2Mg_5Si_8O_{22}(OH)_2$ and $Fe_2Mg_5Si_8O_{22}(OH)_2$ before Al enters the structure (Fig. 8). A hypothetical gedrite end-member, obtained by applying equal proportions of $FeMg_{-1}$ and $AlAl_{-1}MgSi_{-1}$, would contain no Mg and is $Fe_2(Fe_{2.5}Al_{2.5})Al_{2.5}Si_{5.5}O_{22}(OH)_2$. Stout (1971) suggested that the $M(4)$ sites are filled first by Fe before the remaining $M(1–3)$ sites are occupied by equal proportions of Fe and Al. Robinson *et al.* (1971) studied Ca-poor amphiboles from the New Hampshire and Massachusetts area and reported the combination of the two vectors

Ed: $0.5\ NaAl(\square Si)_{-1}$
Ts: $1.5\ AlAl(MgSi)_{-1}$

between the end-members $(Mg,Fe^{2+})_2(Mg,Fe^{2+})_5Si_8O_{22}(OH)_2$ and $Na_{0.5}(Mg,Fe^{2+})_2(Mg,Fe^{2+})_{3.5}Al_{1.5}Si_6Al_2O_{22}(OH)_2$. Their example suggests possible decoupling of the **Ed** and **Ts** vectors in Na-rich amphiboles. Robinson *et al.* (1971) did not discuss the Fe–Mg exchange.

The exchange pattern for the Bushveld case is different. $M(4)$ is not involved, except for the incorporation of small amounts of Na and Fe in the tremolite-rich part of the compositional range. The fact that of five Mg atoms, one is replaced by Fe before Al starts to enter the structure suggests some crystallographic control. It seems reasonable to place Fe^{2+} into the single $M(3)$ site (Hawthorne 1981, 1983). Additional Fe^{2+} is then accommodated by $M(1)$. Data summarized by Hawthorne (1981, Table 24) suggest about an equal preference of Fe^{2+} for $M(1)$ or $M(3)$. Where Al is a *C*-group cation, it is strongly ordered at the $M(2)$ site (Colville *et al.* 1966). If Ti is assigned to tetrahedral sites, equal proportions of Fe and Mg are assigned to the $M(3)$ site, and of Al and Mg to the $M(2)$ sites. If Ti is assigned to octahedral sites, Al in $M(2)$ forms a

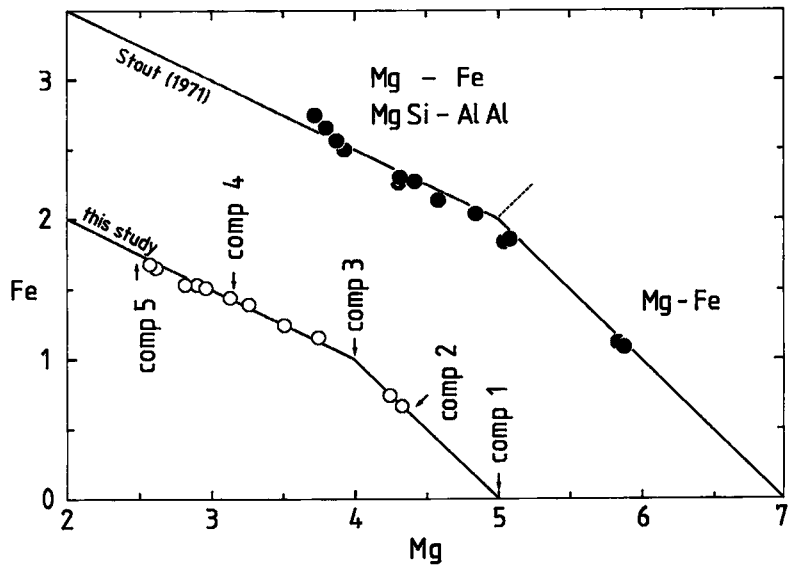

FIG. 8. Variation of Fe *versus* Mg in aluminous cummingtonite from Telemark, Norway (closed circles, Stout 1971) and in compositions from the Bushveld pegmatite (open circles). In both cases, the substitution ratio changes from 1:1 to 1:2 in the high-aluminum part.

fraction of 0.3, and Ti fills the remaining 0.2 sites left by Mg, the fraction of which is 0.5. The increase in size of $M(1)$ or octahedral sites can be accommodated by distortion in the tetrahedral sites (Thompson 1970, Papike & Ross 1970).

The exchange-vector $\diamond_{1.67}Ti_1Fe^{3+}{}_{1.33}Mg_{-4}$ is characterized by cations of similar size (Mg^{2+}: 0.65 Å, Fe^{3+}: 0.67 Å, Ti^{4+}: 0.68 Å). This exchange is confined to octahedral sites. Makino & Tomita (1989) proposed the ordering of these three cations onto $M(2)$. According to Kitamura *et al.* (1975), Ti favors $M(1)$ in oxy-amphiboles. The presence of vacancies in the octahedral position has been proposed for the micas (Forbes & Flower 1974) and pyroxenes (Gasparik 1985), but to the author's knowledge has never been discussed for the amphiboles.

Using the data from Table 3 and introducing trivalent iron, cation plots show an increase in degree of scatter. In particular, the new Fe–Mg diagram has nothing in common with Figure 4. Between key compositions 1 and 3, the 1:1 replacement of Mg by Fe disappears. The following arguments can be used against the presence of trivalent iron in the Bushveld amphibole crystals: a) compositions 1 and 2, which pertain to tremolite needles, show uncharacteristically high values of Fe^{3+} for tremolite, once renormalized; b) the data in Table 3, in which tremolitic amphibole has a similar or even higher content of trivalent iron than its pargasitic counterpart, are in disagreement with the generally higher Fe^{3+} content in brown pargasitic amphibole than is typical in tremolitic amphibole (J. Schumacher, pers. comm. 1989); c) the presence of trivalent iron would dramatically complicate the derivation of exchange-vectors (from Table 3).

Intercrystalline Reactions

In the present section, reactions are derived that are consistent with the observed textures and that are considered responsible for the formation of the Bushveld amphiboles. In the center of the pegmatite, the concentrations of the major elements reach a constant level, suggesting no major influx or removal of cations. The zoning of amphibole in the Bushveld pegmatite follows the disappearance of plagioclase. The disappearance of feldspar and the further production of amphibole causes the tremolite component to increase and the pargasite component to decrease. Phases present in the pegmatite core are: amphibole, clinopyroxene, orthopyroxene, olivine and magnetite. Two reactions are distinguished: one including Na, Al and the pargasite vector, and one excluding those two elements and pargasite. The amphibole composition is given by the mole fraction x (Zingg 1991) in the mineral formula

$$Na_xCa_2Mg_{4-2x}Fe_{1+x}Al_{3x}Si_{8-2x}O_{22}(OH)_2$$

The parameter x includes the **Ed**, **Ts** and $FeMg_{-1}$ vectors in equal proportions. It varies between 0 and 1 and defines the two hypothetical end-members $Ca_2Mg_4FeSi_8O_{22}(OH)_2$ where $x = 0$, and $NaCa_2Mg_2Fe_2AlAl_2Si_6O_{22}(OH)_2$ where $x = 1$.

The changing amphibole composition is taken into account by introducing a reactant and a product amphibole. This leads to equation (1):

$$\underset{\text{Amphibole core}}{Na_xCa_2Mg_{4-2x}Fe_{1+x}Al_{3x}Si_{8-2x}O_{22}(OH)_2} + \underset{\text{Fluid}}{e/2\ O_2 + (a-1)\ H_2O} =$$

$$\underset{\text{Amphibole rim}}{a\ Na_yCa_2Mg_{4-2y}Fe_{1+y}Al_{3y}Si_{8-2y}O_{22}(OH)_2} + \underset{\text{Clinopyroxene}}{b\ CaMg_wFe_{1-w}Si_2O_6}$$

$$+c\ \underset{\text{Orthopyroxene}}{Mg_zFe_{1-z}SiO_3} + d\ \underset{\text{Olivine}}{(Mg_vFe_{1-v})_2SiO_4} + e\ \underset{\text{Magnetite}}{Fe_3O_4} \quad (1)$$

with the stoichiometric coefficients $a = x/y$, $b = 2(1 - x/y)$, $c = [(8v + 2w - 4)(y - x)]/[y(2v - z)]$, $d = [2(2 - 2z - w)(y - x)]/[y(2v - z)]$, $e = [(5z - 2v + 2w - 4)(y - x)]/[3y(2v - z)]$.

In the rocks investigated, the exchange parameter x covers the range $0.5 < Mg/(Mg+Fe) < 0.8$. The stoichiometric coefficients were obtained by mass balance (Zingg 1991, 1992).

Zoned crystals of amphibole in the pegmatite's center are larger than the brown type at the pegmatite's border. Successive zones in the crystals were added to previous ones by growth and dissolution of surrounding pyroxene and olivine. The reaction equation and stoichiometric coefficients suggest two limiting cases: a) There are only two zones at the compositional extreme, x being the composition of the core ($x \approx 0.6$), and y, the composition of the rim ($y \approx 0$). Core and rim are homogeneous and separated by an abrupt and steep discontinuity in concentration. b) The change in element concentration from core to rim is continuous. Each new amphibole zone added to the already existing crystal has a slightly different, more calcic composition than the next inner zone. This is what is observed in the Bushveld rocks.

It is suggested that the amphibole crystals formed in an equilibrium process. The disappearance of plagioclase from the mineralogy and of Na and Al from the rock chemistry, coupled with the further supply of H_2O, caused the breakdown of sodic in favor of calcic amphibole.

On the Mg-rich side, for the interval $0.8 < Mg/(Mg+Fe) < 1.0$, no pargasite is involved, and the only exchange-vector is $FeMg_{-1}$. The reaction is

$$\underset{\text{Tremolite}}{Ca_2(Mg_uFe_{1-u})_5Si_8O_{22}(OH)_2} + e/2\ O_2 = \underset{\text{Clinopyroxene}}{b\ Ca(Mg_wFe_{1-w})Si_2O_6}$$

$$+\ c\ \underset{\text{Orthopyroxene}}{Mg_zFe_{1-z}SiO_3} + d\ \underset{\text{Olivine}}{(Mg_vFe_{1-v})_2SiO_4} + \underset{\text{Magnetite}}{e\ Fe_3O_4} + f\ H_2O \quad (2)$$

with the following stoichiometric coefficients: $b = 2$, $c = (8v + 2w - 5u)/(2v - z)$, $d = [2(2.5u - 2z - w)]/(2v - z)$, $e = (5z - 2v + 2w - 5u)/[3(2v - z)]$, $f = 1$.

It is proposed that this reaction is responsible for the formation of tremolite needles in the pegmatite core (compositions 1 and 2 in Table 2 and 3). Equation (2) does not allow the composition of tremolite to change, which is in agreement with the observation that only amphibole with a fixed ratio Mg/(Mg+Fe) [= 0.855] was found in the tremolite-rich part of the composition range (1 and 2 in Fig. 4).

Summary and Conclusions

Zoned crystals of amphibole allow the quantitative description of intra- and intercrystalline cation-exchange reactions. The compositional difference between core and rim allows the derivation of a bulk exchange-vector. Intercepts and discontinuities in cation plots allow the derivation of elementary vectors. Theoretically, there are different ways to subdivide a bulk vector into elementary vectors. In practice, however, one or at most two choices are realistic. The choice presented in this study is the simplest possible and accounts for generally accepted exchange-vectors. Minor uncertainties in the position of intercepts and key compositions do not affect the type of elementary vectors but cause a slight change in the quantity of vectors on either side of the discontinuity. A different ratio of O:OH results in a parallel shift of a least-squares regression line and therefore does not affect the slope but only the intercept. The calculation of trivalent iron, assuming a cation sum of 13 excluding Ca, Na and K, results in a general increase in the scatter of the data points, the most drastic change being in the Mg–Fe plot. Another argument against trivalent iron in the zoned crystals of amphibole from Bushveld are the almost equal levels of calculated Fe^{3+} between virtually pure tremolite (compositions 1 and 2) and pargasitic brown amphibole (compositions 13 and 14). The amphibole compositions studied tend to deviate only marginally from a basis of 23 atoms of oxygen (B. Leake, pers. comm. 1989).

The major vectors in the case of the Bushveld amphibole crystals follow a simple pattern, with three hypothetical end-members. In a first step, the reaction

$$2\ Cpx_{0.7} + 2\ 7/8\ Opx_{0.6} + 1\ 1/8\ Ol_{0.5} + H_2O + 0.36\ O_2 \rightarrow 1\ Tr_{0.85} + 0.71\ Mag$$

is responsible for the formation of tremolite of a fixed composition along the binary join $Ca_2Mg_5Si_8O_{22}(OH)_2 - Ca_2Mg_4FeSi_8O_{22}(OH)_2$.

The ratio Mg/(Mg+Fe) in tremolite is fixed by the ratio in coexisting olivine, pyroxene and magnetite. These ratios are given as subscripts for the different minerals. Only in a second step is pargasite incorporated into the structure according to the equation

$$Amp_x + 2\ (1 - x/y)\ Cpx_{0.7} + 4\ 2/3\ (1 - x/y)\ Opx_{0.6} + 0.5\ (1 - x/y)\ Ol_{0.5} + (x/y - 1)\ H_2O + 0.25\ (1 - x/y)\ O_2 = x/y\ Amp_y + 0.5\ (1 - x/y)\ Mag.$$

Here, amphibole is allowed to vary in composition between the two end-members $Ca_2Mg_4FeSi_8O_{22}(OH)_2 - NaCa_2Mg_2Fe_2AlAl_2Si_6O_{22}(OH)_2$, disregarding minor components. In both equations, anhydrous silicates are consumed for the transformation and production of amphibole and magnetite. This is in agreement with textures showing magnetite accumulating at the outer rim of zoned crystals of amphibole (Pe-Piper 1988). The simplest exchange-mechanism for the Bushveld amphiboles requires the vector 1.00 $FeMg_{-1}$ between the compositions $Ca_2Mg_5Si_8O_{22}(OH)_2$ and $Ca_2Mg_4FeSi_8O_{22}(OH)_2$.

In the remaining three exchange steps, the vector combining equal proportions of **Ed**, **Ts** and $FeMg_{-1}$

$$NaFeAl_3\square_{-1}Mg_{-2}Si_{-2}$$

is joined by

$$0.05\ FeCa_{-1}$$

between key compositions 2 and 3, by

$$0.05\ \diamondsuit_{1.67}TiFe^{3+}_{1.33}Mg_{-4}$$

between key compositions 3 and 4, and by

$$0.20\ TiSi_{-1}$$

between key compositions 4 and 5.

If more complex processes of exchange are envisaged, it is possible to introduce Ti into octahedral instead of tetrahedral sites, applying the Ti-Tschermak vector $TiAl_2Mg_{-1}Si_{-2}$. Whether Ti is in octahedral or tetrahedral sites does not effect the proposed reaction mechanism, which only accounts for major vectors.

Acknowledgements

The present study has greatly benefitted from discussions and constructive comments by F.C. Hawthorne, T.C. Labotka, J. Laird, G. Pe-Piper, J. Schumacher, E.A. Smelik and F.S. Spear.

References

Burt, D.M. (1988): Vector representation of phyllosilicate compositions. *In* Hydrous Phyllosilicates (Exclusive of Micas) (S.W. Bailey, ed.). *Rev. Mineral.* **19**, 561-599.

Colville, P.A., Ernst, W.G. & Gilbert, M.C. (1966): Relationship between cell parameters and chemical compositions of monoclinic amphiboles. *Am. Mineral.* **51**, 1727-1754.

Della Ventura, G., Robert, J.-L. & Bény, J.-M. (1991): Tetrahedrally coordinated Ti^{4+} in synthetic Ti-rich potassic richterite: evidence from XRD, FTIR and Raman

studies. *Am. Mineral.* **76**, 1134-1140.

FORBES, W.C. & FLOWER, M.F.J. (1974): Phase relations of titan-phlogopite, $K_2Mg_4TiAl_2Si_6O_{20}(OH)_4$: a refractory phase in the upper mantle? *Earth Planet. Sci. Lett.* **22**, 60-66.

GASPARIK, T. (1985): Titanium in ureyite: substitution with vacancy. *Geochim. Cosmochim. Acta* **49**, 1277-1279.

GOLDMAN, D.S. & ROSSMAN, G.R. (1977): The identification of Fe^{2+} in the *M*(4) site of calcic amphibole. *Am. Mineral.* **62**, 205-216.

HARTMAN, P. (1969): Can Ti^{4+} replace Si^{4+} in silicates? *Mineral. Mag.* **37**, 366-369.

HAWTHORNE, F.C. (1981): The crystal chemistry of the amphiboles. *In* Amphiboles and other Hydrous Pyriboles – Mineralogy (D.R. Veblen, ed.). *Rev. Mineral.* **9A**, 1-102.

——— (1983): The crystal chemistry of the amphiboles. *Can. Mineral.* **21**, 173-480.

KITAMURA, M., TOKONAMI, M. & MORIMOTO, N. (1975): Distribution of Ti atoms in oxy-kaersutite. *Contrib. Mineral. Petrol.* **51**, 167-172.

LEAKE, B.E. (1978): Nomenclature of amphiboles. *Am. Mineral.* **63**, 1023-1052.

MAKINO, K. & TOMITA, K. (1989): Cation distribution in the octahedral sites of hornblendes. *Am. Mineral.* **74**, 1097-1105.

PAPIKE, J.J. & CLARK, J.R. (1969): Crystal chemical characterization of clinoamphiboles based on five new structure refinements. *Mineral. Soc. Am., Spec. Pap.* **2**, 117-136.

——— & ROSS, M. (1970): Gedrites: crystal structures and intracrystalline cation distribution. *Am. Mineral.* **55**, 1945-1972.

PE-PIPER, G. (1988): Calcic amphiboles of mafic rocks of the Jeffers Brook plutonic complex, Nova Scotia, Canada. *Am. Mineral.* **73**, 993-1006.

ROBINSON, P., ROSS, M. & JAFFE, H.W. (1971): Composition of the anthophyllite-gedrite series, comparisons of gedrite and hornblende and the anthophyllite – gedrite solvus. *Am. Mineral.* **56**, 1005-1041.

———, SPEAR, F.S., SCHUMACHER, J.C., LAIRD, J., KLEIN, C., EVANS, B.W. & DOOLAN, B.L. (1982): Phase relations of metamorphic amphiboles: natural occurrence and theory. *In* Amphiboles: Petrology and Experimental Phase Relations (D.R. Veblen & P.H. Ribbe, eds.). *Rev. Mineral.* **9B**, 1-227.

SCHIFFRIES, C.M. (1982): The petrogenesis of a platiniferous dunite pipe in the Bushveld Complex: infiltration metasomatism by a chloride solution. *Econ. Geol.* **77**, 1439-1453.

STOUT, J.H. (1971): Phase petrology and mineral chemistry of coexisting amphiboles from Telemark, Norway. *J. Petrol.* **13**, 99-145.

STUMPFL, E.F. & RUCKLIDGE, J.C. (1982): The platiniferous dunite pipes of the Eastern Bushveld. *Econ. Geol.* **77**, 1419-1431.

THOMPSON, J.B., JR. (1970): Geometrical possibilities for amphibole structures: model biopyribole. *Am. Mineral.* **55**, 292-293 (abstr.).

———(1981): An introduction to the mineralogy and petrology of the biopyriboles. *In* Amphiboles and other Hydrous Pyriboles – Mineralogy (D.R. Veblen, ed.). *Rev. Mineral.* **9A**, 141-188.

——— (1982): Composition space: an algebraic and geometric approach. *In* Characterization of Metamorphism Through Mineral Equilibria (J.M. Ferry, ed.). *Rev. Mineral.* **10**, 1-31.

———, LAIRD, J. & THOMPSON, A.B. (1982): Reactions in amphibolite, greenschist and blueschist. *J. Petrol.* **23**, 1-27.

UNGARETTI, L. (1980): Recent developments in X-ray single crystal diffractometry applied to the crystal chemical study of amphiboles. *Godisnjak Jugosl. centre za kristal.* **15**, 29-65.

———, SMITH, D.C. & ROSSI, G. (1981): Crystal-chemistry by X-ray structure refinement and electron microprobe analysis of a series of sodic-calcic to alkali-amphiboles from the Nybö eclogite pod, Norway. *Bull. Minéral.* **104**, 400-412.

VILJOEN, M.J. & SCOON, R.N. (1985): The distribution and main geologic features of discordant bodies of iron-rich ultramafic pegmatite in the Bushveld complex. *Econ. Geol.* **80**, 1109-1128.

WAGNER, C. & VELDE, D. (1986): The mineralogy of K-richterite-bearing lamproites. *Am. Mineral.* **71**, 17-37.

WAYCHUNAS, G.A. (1987): Synchrotron radiation XANES spectroscopy of Ti in minerals: effects of Ti-bonding distances, Ti valence, and site-geometry on absorption edge structure. *Am. Mineral.* **72**, 89-101.

ZINGG, A. J. (1991): Mineral reactions in closed system involving amphibole and plagioclase. *Am. Mineral.* **76**, 617-627.

——— (1992): The formation of a Cpx-corona – mass balance considerations. *Lithos* **28**, 55-68.

Received August 24, 1992, revised manuscript accepted November 25, 1992.